

## MEDIUM FREQUENCY INDUCTION-HEATED CHEMICAL REACTOR WITH COOLING METALLIC ENVELOPE OF THE TANK

J. Nuns<sup>(1)</sup>, B. Paya<sup>(1)</sup>, Y. Neau<sup>(1)</sup>, V. Fireteanu<sup>(2)</sup>, T. Tudorache<sup>(2)</sup>, A. Spahiu<sup>(2)</sup>

<sup>(1)</sup>Electricité de France - R&D Division, Induction Group,  
Moret-Sur-Loing, Route de Sens-Ecuelles, France

<sup>(2)</sup>POLITEHNICA University of Bucharest, EPM\_NM Laboratory  
313 Splaiul Independenței, Bucharest, Romania

**ABSTRACT.** The paper studies a high efficiency induction heated chemical reactor, medium frequency supplied (1000 ... 2000 Hz), able to be equipped with efficient cooling circuits.

Solutions to increase the transparency of the cooling envelope of the reactor tank with respect to magnetic field are studied, based on the 3D finite element analysis of induced currents. The positions of envelope regions characterized by high values of power losses are experimentally confirmed by infrared temperature measurements.

### INTRODUCTION

In the induction-heated chemical reactors called "half-shell" cooling reactors [1] the cooling systems is ensured by a coil, consisting of a stainless steel tube of flattened semi-circular cross section, welded to the outside wall of the reactor tank. This type of reactor with stainless steel tank operate at the network frequency, 50 Hz. Unfortunately, in medium frequency supply (1000 ... 2000 Hz), the cooling system, closer to the inductor, would be preferably heated. Another important drawbacks of the network frequency operation are the high level of vibrations and noises dues to the electromagnetic forces. That is why, this paper studies a medium frequency induction-heated reactor. In comparison with 50 Hz supply, the medium frequency supply increases the electric efficiency and reduces the cost of the inductor, magnetic cores, capacitors and cables.

The optimal design of a medium frequency induction-heated chemical reactor, with a cooling metallic envelope interposed between the reactor tank and the inductor, Fig. 1, can have as support a numerical model able to compute the induced currents in the reactor tank and their cooling envelope. The tank is a heating element of the reactor when the inductor is electrically supplied and can ensure the rapid cooling of

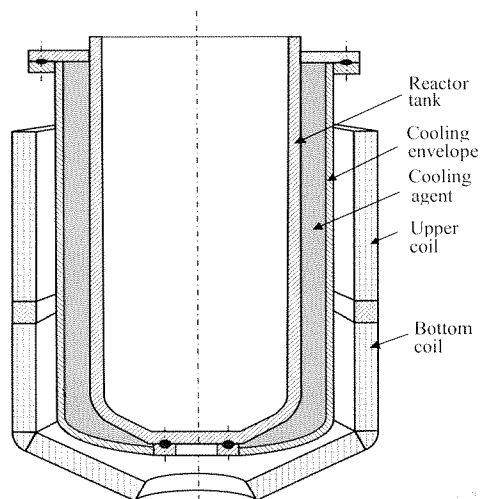


Fig. 1. Induction-heated chemical reactor with cooling envelope of the tank

the processed liquid, if desired [2]. In order to minimize the power losses, the cooling envelope must have high transparency to the magnetic field created by the inductor.

### PHYSICAL MODEL OF A CHEMICAL REACTOR WITH COOLING ENVELOPE

In order to reduce the power losses in the cooling envelope, the regions S1, S2, S3 and S4 in Fig. 2c) are not continuous in azimuthal direction. The segments placed around the reactor tank, Fig. 2a), are separated by longitudinal non-conductive cuts from FL\_SUP to FL\_INF regions, Fig. 2c). The induced current does not pass from a segment to another.

The surface covered by one of the  $n$  segments of envelope in azimuthal direction corresponds to an angle of  $360/n$ . The geometry in Fig. 2 takes into consideration the vertical symmetry of each segment; thus, the induced current density can be computed only on a sector of  $180/n$  from all reactor tank and envelope.

Two short-circuit copper tube rings, water-cooled, SP\_SUP and SP\_INF, Fig. 2c), are placed to the upper and lower extremities of the inductor in order to decrease the power losses in S1 and S4 surfaces of the envelope and to cool the envelope during the reactor heating.

In order to decrease the power losses in the cooling envelope, the vertical cuts UPPER\_CUT and LOWER\_CUT in Fig. 2c) are placed to the extremities of the inductor.

The upper coil of the reactor, Fig. 1, is cylindrical and the lower coil has a conical section that covers a part of the reactor bottom.

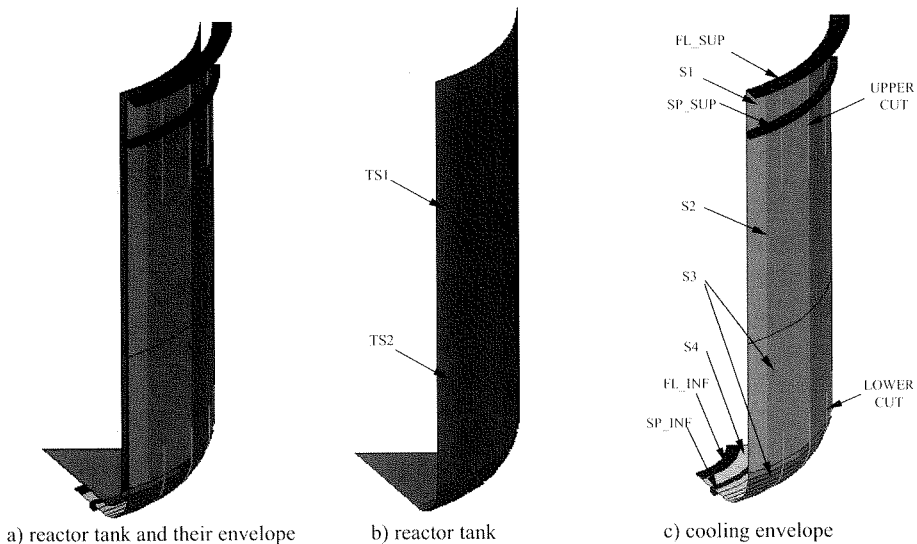


Fig. 2. Regions where the induced currents are computed. Envelope with  $n = 3$  segments and  $m = 7$  cuts per segment

### MATHEMATICAL MODELS FOR INDUCED CURRENTS COMPUTATION

The usual model for induced currents computation is based on the coupling of formulations  $T\Phi - \Phi - \Phi_r$ , in electric vector potential  $T$  and total magnetic scalar potential  $\Phi$  for the conductive regions of tank and envelope, in  $\Phi$  for the non-conductive magnetic cores and in reduced magnetic scalar complex potential  $\Phi_r$  for the rest of regions, non-conductive and non-magnetic.

The equations of the  $T\Phi - \Phi - \Phi_r$  model are as follows:

- for the tank and envelope regions:

$$\begin{aligned} \text{curl}[(1/\sigma) \cdot \text{curl} \underline{T}] + j \cdot \mu \cdot \omega (\underline{T} - \text{grad } \underline{\Phi}) &= 0 \\ \text{div} [\mu \cdot (\underline{T} - \text{grad } \underline{\Phi})] &= 0, \\ \text{div } \underline{T} &= 0, \end{aligned} \quad (1)$$

- for the magnetic core regions:

$$\text{div} [\mu \cdot (-\text{grad } \underline{\Phi})] = 0 \quad (2)$$

- for the air region and the region occupied by the inductor:

$$\text{div} [\mu_0 (-\text{grad } \underline{\Phi}_r + \underline{H}_0)] = 0, \quad (3)$$

where  $\mu$  is the magnetic permeability,  $\sigma$  is the electric conductivity,  $\omega = 2\pi f$  pulsation, and  $f$  is the field frequency. The quantity  $\underline{H}_0$  is the magnetic field created by the inductor current density  $\underline{J}_I$  in the free space, computed by Biot – Savart formula:

$$\underline{H}_0 = \frac{1}{4\pi} \iiint_V \frac{\underline{J}_I \times \underline{r}}{r^3} dV, \quad (4)$$

The density of the induced currents is evaluated by the equation  $\underline{J} = \text{curl} \underline{T}$ .

In case of conductive regions of constant thickness, a specific surface formulation of electromagnetic field [3, 5] can be used for induced current computation. This particular formulation, called *Hyperb\_J\_Conductor* in [5], is much more economic from numerical point of view, because the real volume regions are modeled by surface regions.

### COMPUTATION DOMAIN AND BOUNDARY CONDITIONS

The computation domain of the 3D electromagnetic field, Fig. 3, corresponds to an envelope with  $n = 3$  segments and represents 1/6 of the full geometry, delimited by two axial symmetry planes.

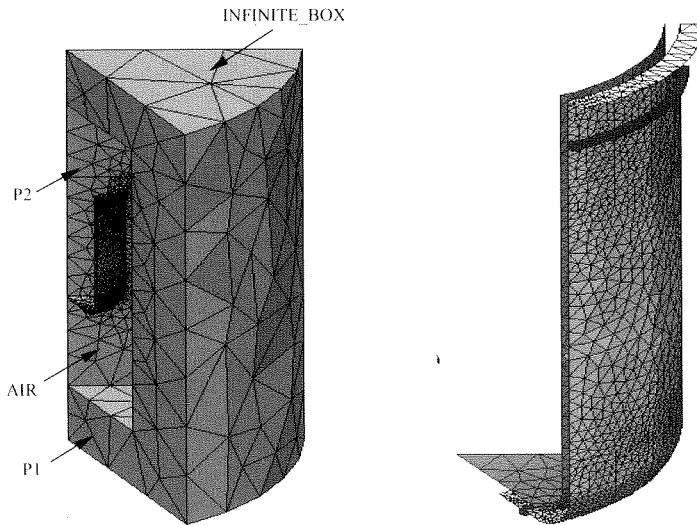


Fig. 3. Geometry and mesh of the magnetic field computation domain

The plane P1, Fig. 2, contains the longitudinal cut that disjoins the successive segments of the envelope, while P2 is the symmetry plane of a segment.

The computation domain includes the surface regions indicated in the Figs 2b) – the tank and 2c) – the envelope and the AIR volume region that includes also the volumes occupied by the two coils of the inductor. The special non-conductive and non-magnetic region, called INFINITE\_BOX in FLUX software [3], models the extension to the infinity of the field domain.

The normal component of the magnetic field vanishes to the boundaries P1 and P2. The condition of null electromagnetic field to the infinity is implicitly considered.

A special boundary condition called CANCELLED\_JUMP [3] is applied to the boundary of the envelope placed in the plane P2, Fig. 2, and to the UPPER\_CUT and LOWER\_CUT line regions in Fig. 2. The normal component of the current density are null on these lines.

## NUMERICAL MODEL OF THE REACTOR

The common input data of the numerical applications analysed in this chapter are:

- outer tank diameter, 600 mm;
- thickness of tank wall, 3 mm;
- outer envelope diameter, 640 mm;
- envelope thickness, 1 mm, except FL\_SUP et FL\_INF, Fig. 2c) of 8 mm thickness;
- resistivity of the conductive regions (stainless steel),  $1 \mu\Omega\text{m}$ , except copper rings;
- relative permeability, 1;
- inner inductor diameter, 676 mm;
- outer inductor diameter, 700 mm;
- reactor tank high, 924 mm;
- position of upper cooper tube ring, 94 mm from the upper extremity of the reactor tank;
- cross section of copper rings, 12 mm x 12 mm, thickness 1 mm and rezistivity  $0.02 \mu\Omega\text{m}$ ;
- mean diameter of lower copper ring, 184 mm;
- position of upper coil of the inductor, 106 mm from the upper extremity of the tank;
- high of the upper coil of the inductor, 420 mm;
- distance between upper and lower coils on the inductor, 40 mm;
- number of turns: 47 on upper inductor coil and 42 on the lower coil;
- current supply, 400 A rms/ turn.

In the acceptance of the reference [5], the tank and the envelope are electromagnetically and geometrically thin regions for frequencies around 2000 Hz. A numerical application in the absence of envelope gives the following values of the power in the tank: 711.6 kW with the  $T\Phi - \Phi - \Phi_r$  volume model and 708.3 kW with the *Hyperb\_J\_Conductor -  $\Phi - \Phi_r$*  surface model. In the first model the mesh of the computation domain contains 62761 nodes, the system to be solved has 169660 equations and the computation time was 4184 s in comparison with 41409 nodes, 47032 equations and only 962 s in the second model. Consequently, this last model was chosen for the numerical simulations further analyzed.

### Results related to a very transparent envelope and comments.

The values of induced power in different conductive zones of the reactor for  $f = 2000 \text{ Hz}$ ,  $n = 3$  segments,  $m = 3$  upper and lower cuts per each segment, 50 mm length of the upper cuts in the S1 area, Fig. 1, and 150 mm in the S2 area, and 186 mm length of the lower cuts in S3 area and 15 mm in the S4 area, are as follows:

- 698.64 kW useful power in the reactor tank;
- 0.271 kW in the FL\_SUP area of the envelope;
- 2.267 kW in the S1 area of the envelope;
- 3.680 kW in the S2 area of the envelope;
- 4.807 kW in the S3 area of the envelope;

- 0.489 kW in the S4 area of the envelope;
- 0.088 kW in the FL\_INF area of the envelope;
- 1.066 kW in the upper cooling ring, SP\_SUP, of the envelope;
- 0.246 kW in the lower cooling ring, SP\_INF, of the envelope.

The power losses in all reactor envelope, only 12.91 kW, characterise a very transparent cooling envelope, because these losses represents only 1.81 % of the total induced power.

The chart and patterns of the induced current density in such an envelope are presented in Fig. 4.

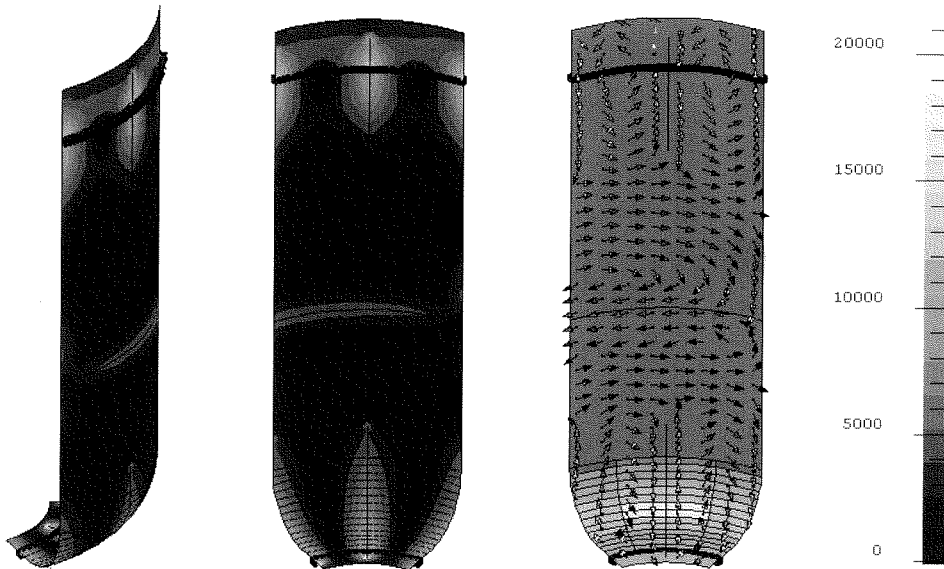


Fig. 4. Chart and patterns of the induced current in the envelope

Influence of the number of envelope segments.

The maximum value of the induced current density, Fig. 5, decreases when the number of segments increases.

The increase of the number  $n$  of envelope segments, Table 1, determines the decrease of ratio between the power losses and the total induced power. The power induced in the reactor tank (column TANK in Table 1) increases only some percents, while the decrease of the power losses in the envelope (ENVP column) is more important.

Table 1. Induced power in different conductive regions of the reactor in [kW]

Nb. of segm.	TANK	FL_SUP+ FL_INF	SP_SUP+ SP_INF	S1	S2	S3	S4	ENVP	ENVP/(TANK+ENVP)
n = 2	639.60	8.19	1.67	4.60	15.58	33.75	2.40	66.19	9.38 %
n = 3	660.00	4.59	1.50	4.63	12.44	26.60	1.41	51.17	7.20 %
n = 4	672.10	2.71	1.40	4.39	10.45	20.57	1.74	41.26	5.78 %

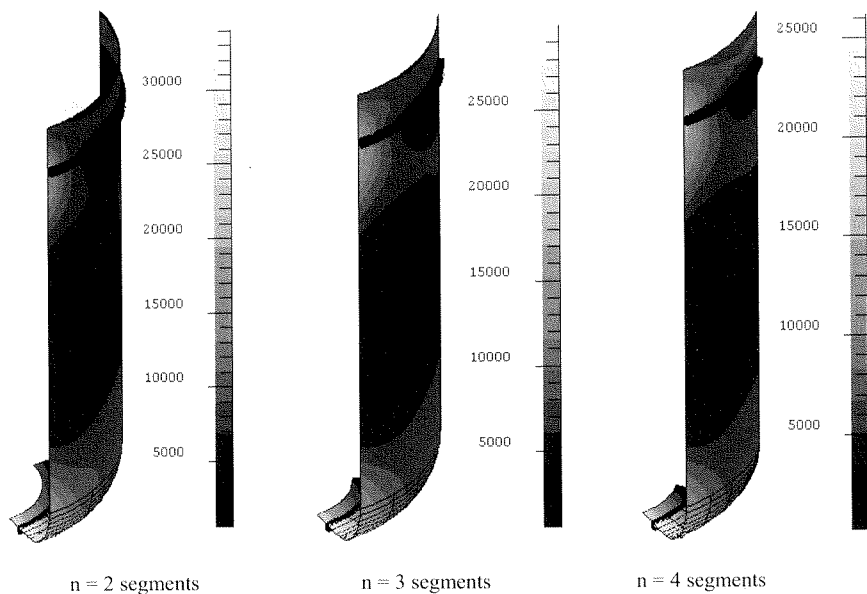


Fig. 5. Chart of current density in the envelope

Vertical cuts in the envelope segments.

The presence of vertical cuts in the envelope segments, Fig. 6, in the area of upper and lower copper rings, Fig. 2c), ensure the decrease of the power losses in the envelope, Table 2. In the same time, the power in the tank slightly increases. A number of  $m = 3$  cuts per segment leads to the decrease of the ratio power losses/total induced power in comparison with the envelope without cuts from 7.29 % to only 1.81 %.

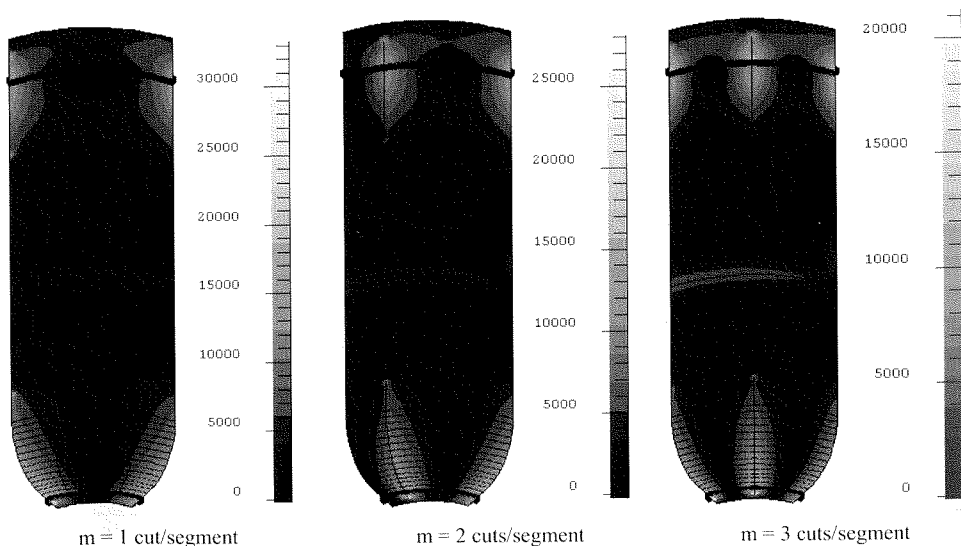


Fig. 6. Chart of induced current density in the envelope

Table 2. Induced power in [kW] ( $n = 3$ ) for different numbers of cuts per segment

Cuts per segment	TANK	ENVP	ENVP/ (TANK+ENVP)
$m = 0$	660.00	51.17	7.20 %
$m = 1$	685.55	28.37	3.97 %
$m = 2$	694.11	18.59	2.61 %
$m = 3$	698.65	12.91	1.81 %
$m = 5$	700.93	9.47	1.33 %
$m = 7$	703.06	6.31	0.89 %

Table 3. Induced power in [kW] for different frequency values

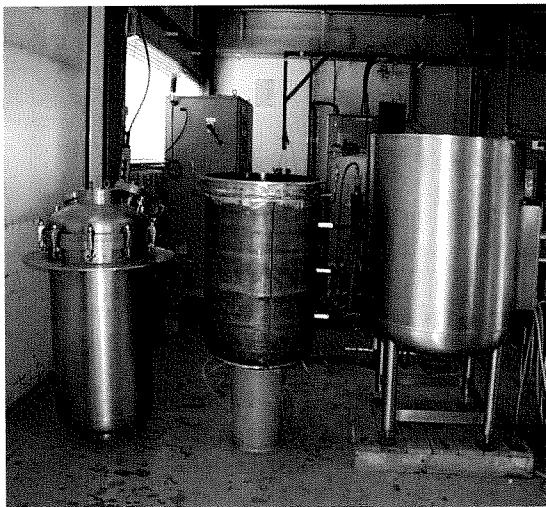
Freq. [Hz]	TANK	ENVP	ENVP/ (TANK+ENVP)
1000	638.44	6.96	1.08 %
2000	698.65	12.91	1.81 %
3000	711.54	20.36	2.78 %

Supply frequency influence.

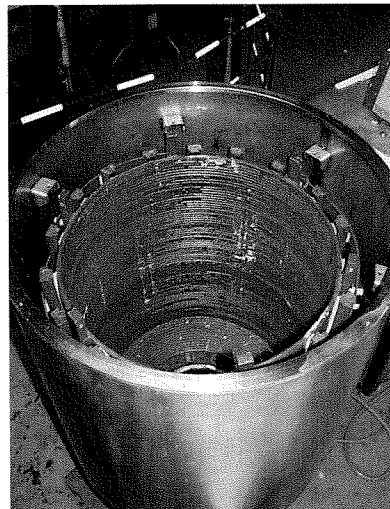
The increase of the frequency leads to the increase of the relative power losses. The results in Table 3, correspondent to  $n = 3$  segments and  $m = 3$  cuts/segment, show a much more important increase of the power losses in the envelope than the increase of the useful power, induced in the tank.

**EXPERIMENTAL VALIDATION**

Experimental researches was accomplished by the Induction Laboratory, R&D Division of Électricité de France on a test reactor of 250 liters, Fig. 7, whose characteristics correspond to the previously computation data. The envelope of the tank, in the middle of the Fig. 7 a), has 3 segments without cuts ( $m = 0$ ). The vertical separation between the three segments of the envelope extends only between the two copper rings. In the numerical model this separation is longer, between the two extreme areas FL\_SUP and FL\_INF, Fig.1.



a)



b)

Fig. 6. Chemical reactor of 250 l, tested by Électricité de France

The right side image of the Fig. 6a) and the Fig. 6b) include the protection envelope and the inductor. A number of 18 vertical magnetic cores, of low frequency ferrite bars, are equidistant placed around the inductor.

### Testing results and comparison with numerical results.

A low power supply test (20 kW ... 40 kW), for three different frequencies, 1040, 1720 and 3140 Hz, was performed to evaluate the electrical efficiency of the reactor. The main results are the following:

- a) in the absence of the cooling envelope, a value of efficiency around 95 % was determined. Consequently, the power losses in the inductor represents 5 % of the total power;
- b) when the frequency increases, the relative value of power losses in the envelope increases. The total power losses – in the inductor and in the envelope, represents around 17 % from total supplied power, for 1720 Hz, and 27 % for 3140 Hz that represents an increase of 59 %. This result is concordant with the numerical model result in Table 3, where the increase of relative value of power losses in the envelope when the frequency increase from 2000 Hz to 3000 Hz is 53.6 %;
- c) for the frequency 1720 Hz, the value of 83 % of electric efficiency was evaluated. It results that the power losses in the envelope represent  $17 - 5 = 12$  % of the total power. The correspondent result of the numerical model is only 7.5 %.

All results previously analyzed correspond to an inductor without magnetic cores. When their presence is considered in the numerical model, an increase of the power losses with about 1.5 % was evaluated. The difference that rests between the experimental results and the numerical results, of about 3 %, comes from the fact that the numerical model does not reflect the real surface contact between the copper rings and the envelope. In the numerical model this surface is considered to be in copper made. In reality, the copper tubes are not in a perfect electric contact with the envelope and consequently, the real power losses in this region are higher than the computed values.

## CONCLUSIONS

The finite element analysis and the experimental investigations on induced power distribution in the tank of a chemical reactor medium frequency heated (1000 ... 2000 Hz) and in their cooling metallic envelope show the possibility to implement efficient cooling circuits in chemical reactors without affecting the performances of the induction heating process.

The optimization of the cooling envelope design concerning the number of its sectors around the tank and the presence of longitudinal cuts at the extremities of the inductor can ensure a reduced level of power losses generated by the induced currents. Thus, with medium frequency supply and a high transparent metallic envelope of the tank, it is perfect possible to built chemical reactors with global efficiencies around 90 %, higher than all actual induction heated chemical reactors, with very efficient cooling of the tank, with lower impact on the working environment and at lowest costs.

## REFERENCES

- [1] CFE/UIE (1997) Electromagnetic Induction and Electric Conduction, *Electra Edition*.
- [2] Marchand, C., Coevoet, M. (1993). Les reacteurs chimiques à induction, *Les Cahiers de l'Ingenierie*, no. 48.
- [3] CEDRAT (2002). Using regions of HYPERB\_J\_CONDUCTOR type, *FLUX User's Guide*, Vol. 4.
- [4] Fireteanu, V., Nica, O (2001). Simulations 2D et 3D du four de purification Carbone Lorraine, *Rapport contract recherche*.
- [5] Fireteanu, V., Paya, B., Nuns, J., Tudorache, T. (2002). Eddy currents in Thin Plates Modeled as Surface Regions, *COMPEL Journal*, Vol. 21, No. 4.